MARSCHNER REVIEW

Deposition rates in growing tissue: Implications for physiology, molecular biology, and response to environmental variation

Wendy K. Silk · Marie-Béatrice Bogeat-Triboulot

Abstract

Background Net rates of biosynthesis and mineral deposition are needed to understand the physiology and molecular biology of growth and plant responses to environmental variation. Many popular models ignore cell expansion and displacement. In contrast, the continuity equation, used with empirical data on growth velocity and concentration, allows computation of biosynthesis and deposition rates in growing tissue.

Scope This article describes data and methods needed to calculate deposition rates and reviews some insights into environmental physiology and molecular biology.

Conclusions Growth zones actively and strongly deposit mineral elements, even though local concentrations may not be changing in time. Deposition rate profiles give important insight into the mechanism of plant responses to drought and salinity, and they clarify many aspects of nitrogen metabolism in roots and leaves. This approach is also essential to understand molecular regulation of growth. A pioneering study determined transcript densities and calculated rates of change in gene expression; this study revealed how *Actin 11* is highly regulated by a balance of transcription and decay during growth of roots. New technologies (*in planta* cytometry, coupled with powerful computational routines and real-time confocal microscopy) will allow determination of deposition rates in growing organs and advancement in understanding of gene regulation.

Responsible Editor: Philippe Hinsinger.

W. K. Silk (✉)
Department of Land, Air and Water Resources,
University of California at Davis,
Davis, CA 95616, USA
e-mail: wksilk@ucdavis.edu

M.-B. Bogeat-Triboulot
INRA, UMR1137 Ecologie et Ecophysiologie Forestières,
54280 Champenoux, France

M.-B. Bogeat-Triboulot
UMR 1137, Ecologie et Ecophysiologie Forestières, Faculté des Sciences et Technologies, Université de Lorraine,
54500 Vandoeuvre-les-Nancy, France

Introduction

Plants grow throughout most of their lives, and they use growth to acquire light, nutrients, and water. Organic compounds are metabolized and mineral elements are deposited in plant cells throughout the cellular development, maturation, and senescence. Net rates of biosynthesis and mineral deposition are needed to understand physiology and the response to environmental variation. Particularly in growing tissue it is necessary to consider expansion and displacement of cells relative to observed concentration patterns.

This is because, in contrast to mature tissues, growing tissue has concentration profiles that are produced by cell expansion as well as nutrient import, catabolism and anabolism, thus, quantitative analyses of morphogenesis are required.

Plant computational morphodynamics is now a popular field of study. The classical literature on plant growth analysis is well cited. Landmark papers include an analysis of cell division rates based on a form of the continuity equation (Goodwin and Stepka 1945), the use of streak photographs by Erickson and Sax (1956) to quantify the one-dimensional growth rate pattern in corn roots, and a quantitative two-dimensional analysis of leaf growth (Erickson 1966). The important distinction between spatial and material (cell-specific) aspects of plant development was clarified three decades ago (Silk and Erickson 1978, 1979; Gandar 1983a, b). More recently Kwiatkowska and Dumais (2003) provided a quantitative analysis of apical morphogenesis, while improved computer-assisted tracking of natural marks has facilitated high-throughput growth analysis at high resolution (Walter et al. 2002; Grandjean et al. 2004; Reddy et al. 2004; Miller et al. 2007). At a recent workshop scientists showed time-lapse images from confocal microscopy of living tissue and described how image analysis is facilitated by genetic transformation to introduce fluorescent markers into plant cells (reviewed in Cunha et al. 2012, images viewable at http://www.computableplant.org/).

And yet in 2012, many computational models are time dependent but neglect to consider growth. Perhaps this is the heritage of the influential Turing model (1952) for morphogenesis. Turing showed that when two or three reactants with different diffusivities are involved in a common chain of chemical reactions, then a small amount of noise leads to stable, inhomogeneous patterns that are suggestive of biological patterning. This has been an appealing approach for theoretical biologists; by 2012 Turing's paper had 3428 citations. However, the Turing models do not include expansion or active sinks both of which characterize growing plant organs. Another popular model, often used for mineral uptake in plants, is based on the Michaelis-Menten equations (1913) for enzyme kinetics. The Michaelis-Menten model assumes a well-stirred beaker: The system is seen to vary in time and to lack spatial gradients. This is not an appropriate

pair of assumptions for a plant. The simplest model plant, in an appropriate (moving) reference frame, has spatial patterns of growth, anatomy, and biochemistry that may not change in time. The model plant must however have spatial variation associated with the developmental gradient, that is, the variation in tissue age at different positions.

By neglecting growth we are missing a major aspect of the ability of sessile organisms to respond to their environment. Continuity equations provide a way to couple growth velocity fields v with patterns of element concentration ρ in space and time, t, to improve mechanistic understanding of the interaction of growth processes and chemistry (Silk and Erickson 1979). In general the local deposition rate, d in a tissue can be calculated from

$$d = \frac{\partial \rho}{\partial t} + \nabla \bullet (\rho \upsilon) \tag{1A}$$

which can be expanded to

$$d = \frac{\partial \rho}{\partial t} + \rho(\nabla \bullet \upsilon) + \upsilon \bullet \nabla \rho \tag{1B}$$

When the deposition rate is positive, the location is a sink for the material of interest. The material can be imported or be produced by local metabolism. A negative deposition rate means the location is losing material by catabolism or by export either to the environment or to other plant tissues. The local deposition rate is a net accumulation rate, the result of synthesis, import, degradation, and/or export.

This article reviews deposition rates in plant tissue and some implications for physiology, ecology and molecular biology. The use of this approach to quantify cell division rates and the molecular regulation of cell division has been reviewed elsewhere (Fiorani and Beemster 2006); environmental effects on coordination between division and elongation have been reviewed by Tardieu et al. (2011). The article concludes by citing some recent computational advances that have the potential to greatly extend understanding of biochemistry and molecular biology of growing tissue.

Technical aspects

Non-growing tissue—seeds and mature tissue When growth is not occurring, the plant tissue may be assayed like a test tube or well-stirred beaker. In a stationary

(conventional) reference frame the growth velocity terms are zero, so that only the first term on the right hand side of the continuity equation is relevant:

$$d = \frac{\partial \rho}{\partial t} \qquad\qquad\qquad (1C)$$

Equation 1C tells us the deposition rate equals the observed rate of change in concentration. It would be assayed for instance in a spectrophotometric assay by a change in color intensity. In the Bradford assay using Coomassie Brilliant Blue dye, an increase in blue color would indicate protein production; a decrease in blue color would indicate destruction of the protein. Seeds and non-growing tissue producing or degrading protein without changes in volume can be characterized in this way.

One-dimensional, steady cases—growing roots and monocot leaves To find the spatial pattern of deposition rates within growing tissue we must know not only the time rate of change of the metabolite at locations of interest, but also the tissue expansion rate and the displacement of the tissue relative to the spatial pattern. A one-dimensional example is suitable for many problems involving roots, monocot leaves, or internodes,

$$d = \frac{\partial \rho}{\partial t} \qquad + \rho\left(\frac{\partial v_z}{\partial z}\right) \qquad + v_z \frac{\partial \rho}{\partial z} \quad (1D)$$

Deposition rate = Local rate + growth dilution + convective
                  of change   rate of change

This equation is derived from the assumption of conservation of matter (e.g. Boas 2005). Here the deposition rate, perhaps in ng per mm of tissue along a plant axis, is a local rate ascribed to a particular position. The equation is in terms of changes in concentration with respect to time, t, and distance, z. We see that the equation needs data on both concentration and growth. To find the spatial pattern of growth velocity, v_z, it is convenient to use the reference frame with origin at a root or shoot apex, or the base of a monocot leaf. That is, $z=0$ and $v_z=0$ at the origin and v_z increases with z to reach a maximum displacement velocity at the base of the growth zone (Erickson and Sax 1956). The velocity gradient is the "relative elemental growth rate" ("REGR") quantifying the local expansion. In this moving reference frame, in the simplest case, growth patterns may be steady (unchanging in time), while cells are formed and displaced through the growth zone (Erickson and Sax 1956; Boffey et al. 1980). In growing roots and monocot leaves the spatial pattern in mineral content may also be steady (Silk and Erickson 1979). The gradient terms may be evaluated in spreadsheets using Erickson's midpoint differentiation
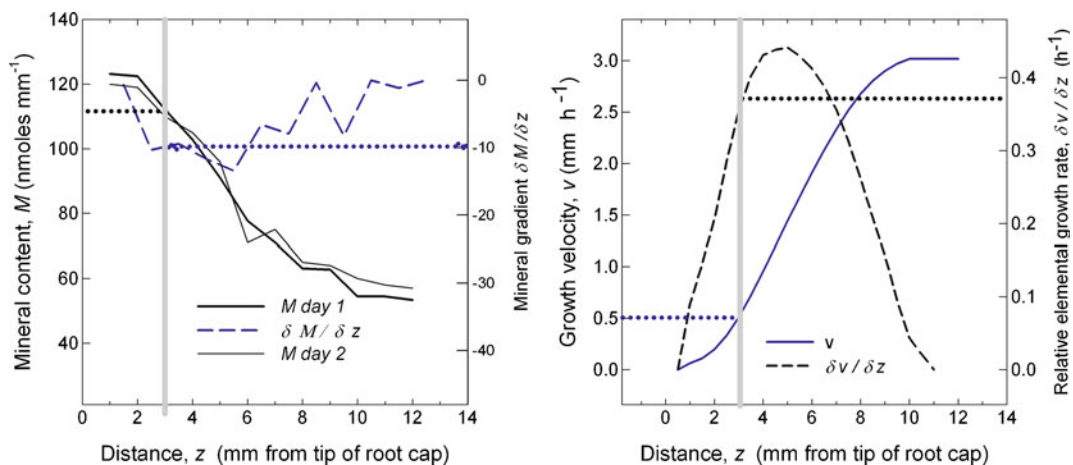

Fig. 1 Data to calculate the deposition rate of a mineral element in the elongation zone of a corn root. (Left—content data) One – mm segments are collected by position and assayed for mineral content in young root tips (*solid black line*) and roots one day older (*thinner solid line*); the curve of content is differentiated with respect to position (*dashed blue line*) to obtain the concentration gradient. (Right—growth data) Observation of mark positions at 15 min. intervals permits calculation of growth velocity (*solid blue line*) and differentiation of the velocity to obtain the velocity gradient ("REGR") as a function of position. At any given location (the *gray vertical line* shows the three mm position) the product of values of the components in *black* are summed with the product of the components in *blue* to calculate the value of the deposition rate

formulas (Erickson 1976), or cubic splines may be fit to the data and numerically differentiated, for instance using MATLAB (The MathWorks, Inc.).

Figure 1 gives an example showing the data needed to calculate the deposition rate in a root tip growing in steady state. Experiments are needed to determine (left) mineral concentration ,with calculated concentration gradient, and (right) growth velocity, with calculated velocity gradient. Here we find that the local rate of change in mineral concentration is negligible. For instance, at the location three-mm from the root tip we find 112 ng of a mineral element whether we look at a young or older root (Fig. 1). We can thus neglect the first term, the local (site-specific) rate of change in concentration. Although the concentration profile was found not to change in time, the remaining terms of Eq. 1D tell us that mineral deposition is certainly occurring. The second term of the equation, the "growth dilution" term, is the product of the local mineral concentration and the

REGR. It is easy to believe that if the tissue is expanding 38 % per h at the location 3 mm from the root tip, then the tissue element must be depositing 38 % of 112 ng, about 42 ng, each hour to maintain the observed local concentration of the mineral element, 112 ng per mm. The last term of the equation, the "convective rate of change," is harder to grasp. An analogy makes it easier to see as the term needed to maintain an observed gradient in concentration (Fig. 2).

The growth dilution term is always positive in growing tissue. The convective rate of change is negative if the concentration decreases with position (a negative gradient as in Fig. 1), and positive if concentration increases with position so that the tissue element increases in concentration during its displacement (as suggested in Fig. 2). The experimental design used to obtain Fig. 1 gives results per mm of root or leaf. These results can be made more universal if they are divided by the weight or cross-sectional area of the segments used for the

Fig. 2 Analogy to visualize the concept of the convective rate of change. (Above) Imagine that an artist wants to paint a school of fishes swimming in a stream. The problem is how to maintain the pattern of fishes long enough to paint it. (Below) An answer to this problem is that the artist can hire workers to throw fishes into the stream. The faster the fish are moving, the more rapidly the workers must add new fish. And the greater the difference in fish between locations, the more rapidly the workers must throw in the new fish. This analogy suggests the logic of the convective term, the product of velocity and spatial gradient (change with position) in concentration

$$v\frac{\partial \rho}{\partial x}$$
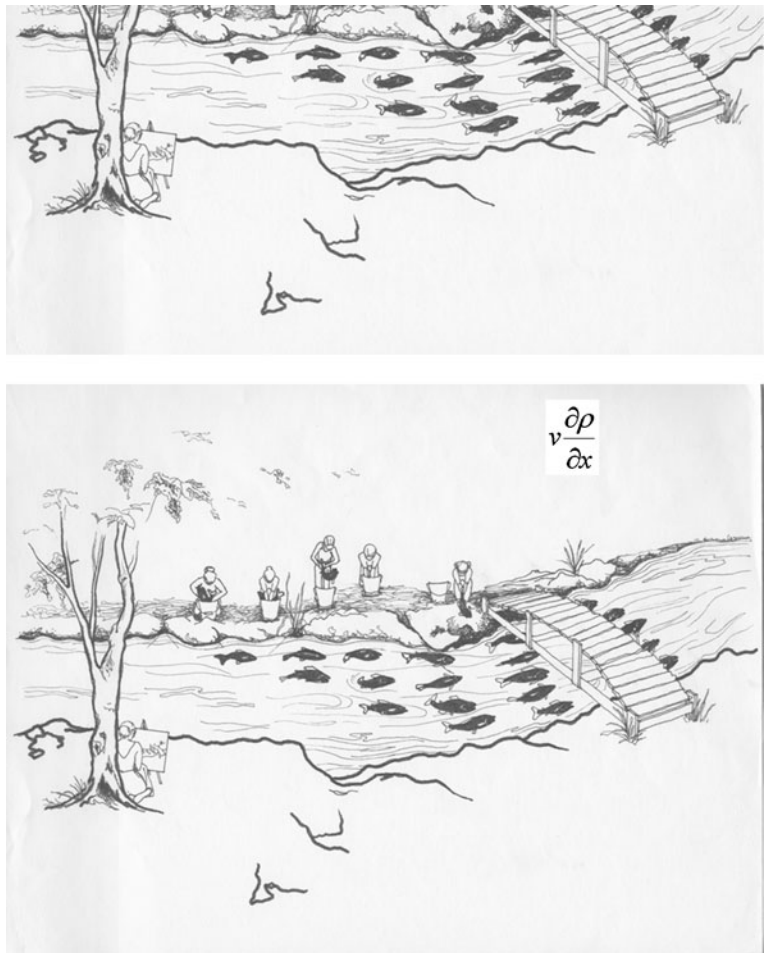
chemical assay, to give deposition rates on the basis of tissue weight or volume (Silk et al. 1984).

Sampling and time intervals The continuity equations show that the spatial patterns of growth velocity and metabolite concentration are the basic data required to find the metabolite deposition rates. Tissue sampling should provide adequate resolution through the growth zone. Indeed linear growth zones show a large range of length. Determining metabolite concentration profiles is easier in long growth zones without needing to pool samples. Recently, Nelissen et al. (2012) used the 65 mm-long growth zone of the maize (*Zea mays* L.) leaf to facilitate the determination of several hormone concentrations. The ~30 mm-long growth zone of grasses such as tall fescue (*Festuca arundinacea* Schreb.) leaf offer also a good model (Schnyder and Nelson 1988; Gastal and Nelson 1994). A mm-scale resolution is required for plant roots whose growth zone is around 10 mm such as maize (Sharp et al. 1988) or poplar (*Populus deltoïdes × nigra* cv. 'Soligo') (Merret et al. 2010). The shorter root growth zone of the model plant *Arabidopsis thaliana* (L.) Heynh. (~2.5 mm, Beemster and Baskin 1998) requires much higher resolution, using microdissection or imaging of quantitative and sufficiently short-lived reporters. At the other end of the size scale, the giant blades of bull kelp (*Nereocystis luetkeana* (K. Mertens) Postels & Ruprecht) have growth zones almost one meter long and can be sampled on the 5-cm scale (Koehl et al. 2008).

For the growth analysis, the movement of natural or applied marks should be followed on a time scale long enough for mark displacement, but short enough that marks do not move too far from their initial, ascribed positions (Silk 1984). A rule of thumb is that the time interval for observation should be chosen so that marks do not move more than 15 % of the length of the growth zone. To capture the growth near the origin (where growth velocity is small), it may be useful to follow the marks over a longer time scale than that used to analyze the faster moving marks. Ideally, the sampling time scale should be adequately designed to also assess shorter temporal variations-hourly oscillations and circadian rhythms (Merret et al. 2010).

Comparison to radiolabel experiments The deposition rate computed with data on growth velocity and chemical concentration would be expected to parallel the results of an uptake experiment in which the tissue is incubated with radioactive label. Results are not in general numerically comparable, since the continuity equation returns endogenous deposition rates, while the labeling experiment shows deposition of the exogenous supply. Still, to understand nutrient uptake in roots, a label experiment can give valuable information if an appropriate time scale is chosen for the uptake experiment. Problems in experimental design arise because the radioactive labeling experiment is not instantaneous (Silk et al. 1984). Some time is required for penetration of the label into the tissue, and during this time interval the cells found at one location will be displaced to another. For instance in the corn roots of the study on uronide deposition, cells
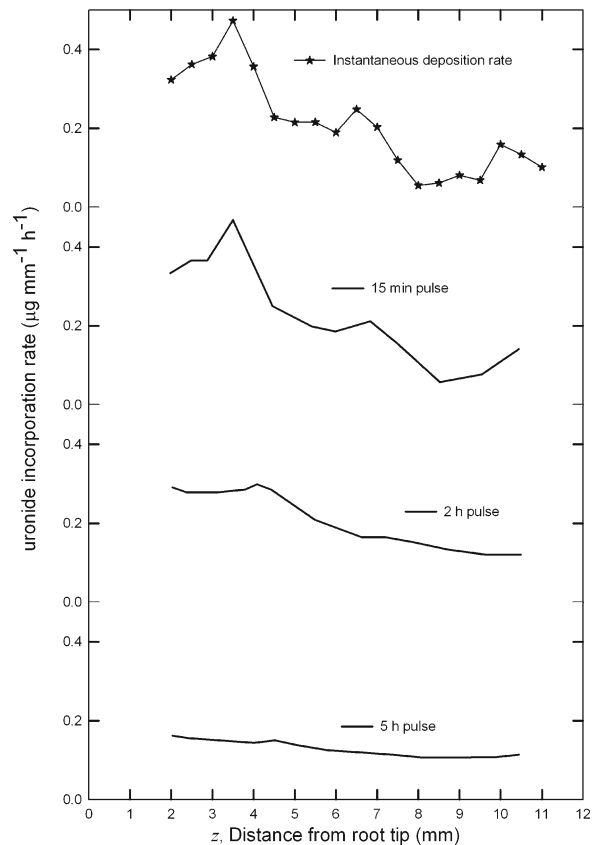

Fig. 3 Numerical simulation of radiolabel incorporation experiments. *Upper line* shows the calculated deposition rate of uronide. *Lower lines* show profiles of radioactive incorporation that would be apparent after progressively longer periods of incubation in radiolabel. Redrawn from Silk et al. (1984) Uronide Deposition Rates in the Primary Root of Zea-Mays. Plant Physiology 74: 721–726, www.plantphysiol.org, Copyright American Society of Plant Biologists

found initially at 4 mm will be located an hour later at 5.2 mm, where the deposition rate is quite different. As the time interval of the labeling period is increased, the discrepancy increases between the instantaneous deposition rate and the apparent label incorporation rate (Fig. 3). The cells at the sampling locations have arrived from progressively more apical locations, and their label integrates the deposition rates they have experienced in space and time. Numerical experiments show that a 15 minute pulse of radio-label will return a trend similar to a calculated deposition rate (Fig. 3). But a two h pulse will not reveal the peak of the instantaneous pattern, and by five h the incorporation rate pattern appears flat (uniform), in great contrast to the pattern revealed by the continuity equation. The take home message is that the criteria for accurate growth analysis should be applied to a radio-label experiment: the duration of incubation in label should be short relative to the growth displacements of the tissue.

Lagrangian (cell-particle-specific) description Most of the time, concentration and net deposition rate are given as a function of position in the growth zone and describe "what happens" in each particle or cell disposed along the growth zone. It is also interesting to get a temporal and spatial description of these variables in a single particle or cell cohort crossing the growth zone as time goes on (Green 1976; Silk and Erickson 1979; Gandar 1983a, b). This cell-specific description is called a *Lagrangian* specification as opposed to the spatial (site-specific) or *Eulerian* specification (Silk and Erickson 1979). If data are given as spatial patterns of a developmental variable, to follow a cell requires determining the Eulerian specifications

of growth and of the variable over the time necessary for a particle to cross the growth zone. In non-steady state this requires extensive data on spatial and temporal patterns of the variable and the growth velocity. In steady state (that is, if spatial patterns of both growth velocity and density are not changing with time), the spatial specification can be interpreted as descriptions of "what happens" in a single particle as it is moved through the growth zone. In steady state it is also possible to use a single growth velocity curve to determine the growth trajectory, that is the relationship between particle position and time, from the temporal integration of the velocity field following the particle (Silk and Erickson 1979; Gandar 1983a) or by counting cells outside the meristem (Silk et al. 1989). Then the spatial coordinates can be converted into temporal coordinates to provide the Lagrangian specification.

By displaying the hidden temporal aspects of growth, Lagrangian specifications provide new information. For instance, in maize and pine (*Pinus pinaster* Aiton) roots, osmotic stress affected relative elemental growth rate pattern (REGR) according to the stress level. It shortened the length of the growth zone (Sharp et al. 1988; Triboulot et al. 1995). Drawing the Lagrangian REGR profiles revealed that duration of longitudinal expansion was similar for all stress levels (Sharp et al. 1988). More recently this approach has been applied to molecular biology. Merret et al. (2010) determined the Lagrangian specification of *Actin* transcript density (Fig. 4) in roots of poplar. This analysis revealed the long temporal extent of the apical peak and the relatively short duration of the more basal peak. A 3D-plot where both time and space are plotted is another graphical way to show these two points of view (see a rotation 3D-pot at http://www.biomedcentral.com/1741-
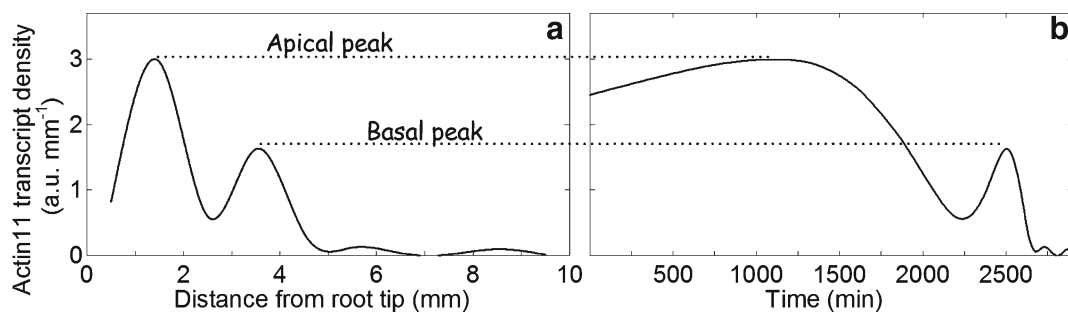

Fig. 4 Actin11 transcript density (a.u.mm^{-1}) as a function (**a**) of position along the primary root apex of poplar and (**b**) of time in an element positioned initially at 1 mm and moving across the growth zone (from Merret et al. 2010)

7007/8/18/additional). In general, determining the La-grangian specification of transcript densities and gene products is an exciting and unexplored approach for understanding the molecular biology of response to environmental variation.

As applied in Fig. 4, the classical way consists of drawing the growth trajectory of a particle initially positioned near the meristem as it is moved toward the distal positions by the elongation of younger cells. However it is also possible to go back in time and to determine the growth trajectory of a particle that finishes its route at a determined final position. Figure 5 shows the "reverse" growth trajectories of particles spread every 0.25 mm along the growth zone of a poplar root apex (drawn from Merret et al. 2010). The interesting point is that, 20 h before, these particles were all positioned in the segment [1–1.75 mm]. Thus drawing the temporal specification for particles reaching a range of final positions may be also useful for comparing treatments affecting the length of the growth zone.

Biological outcomes: Regulation of metabolite concentration in growth zones

In this section we describe some basic patterns that emerged during early applications of the continuity equation to analyse metabolite production in growing tissue. A later section on biological outcomes then quantifies impacts of environmental variation.

The pattern of metabolite density may be unchanging with time in primary growth zones while the cellular population of the zone is replaced several times In the 1980s, the Silk laboratory showed that the uronide concentration profile in young maize roots is similar to the concentration profile in roots 15 h older. Figure 6 (redrawn from Silk et al. 1984) shows the uronide concentration profile in the elongation zone above the meristem (1.5–11 mm from the root tip). A separate growth analysis revealed that the cellular population of this zone was replaced twice during the 15 h period. In both young and older roots, the uronide in each tissue element falls from 1.4 µg mm^{-1} to 0.8 µg mm^{-1} as the tissue is displaced through the growth zone. In general in roots and monocot leaves the concentration profiles are often quasi-steady,
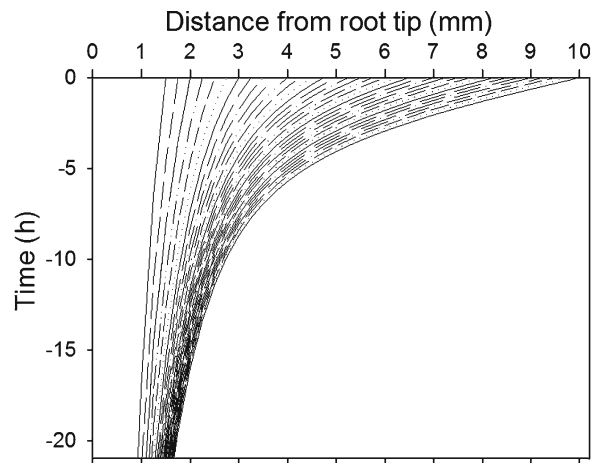

Fig. 5 Reverse trajectories of particles spread every 0.25 mm along the growth zone at $t=0$, for the 20 preceding hours (drawn from Merret et al. 2010)

changing only slowly relative to the displacement of the cells through the profile.

Even when the concentration of a mineral element is decreasing in developing tissue, large deposition of the element is occurring. Growth zones are often the largest sink for metabolites and mineral elements The Fig. 7a and b show that potassium concentration decreases during root development. This is seen in two different ways. Cells lose potassium concentration as they are displaced through the growth zone—compare $[K^+]$ at 2 and 10 mm from
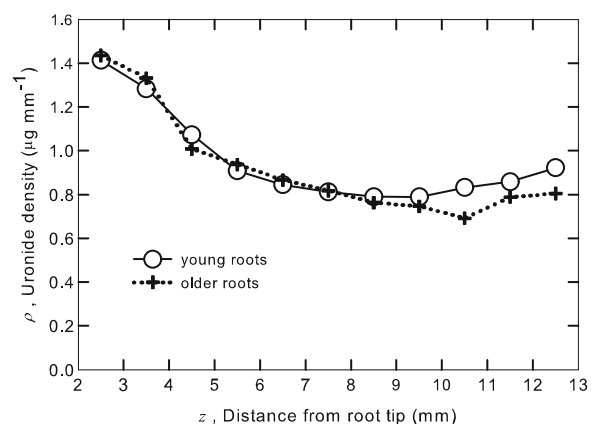

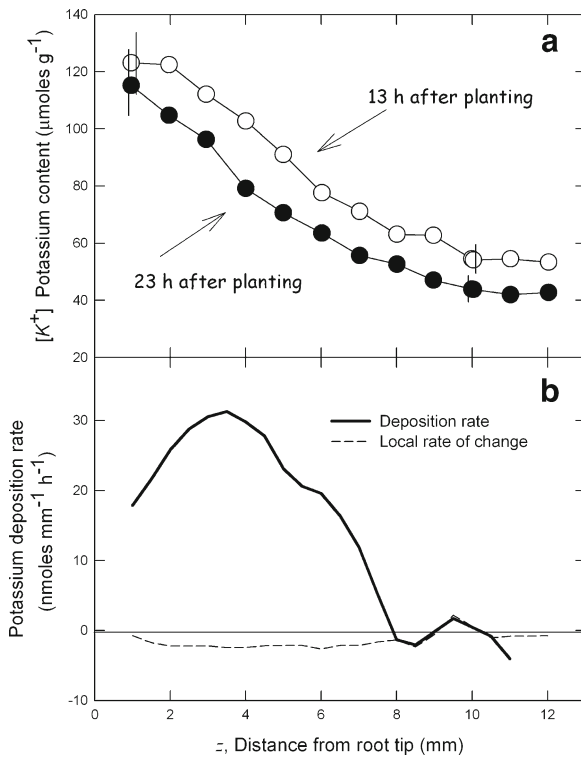**Fig. 6** Profiles of uronide density in young and older root tips of maize seedlings. Citation as in Fig. 3

Fig. 7 Profiles of **a**) potassium density and **b**) large positive potassium deposition rate and the small component, the local rate of change in potassium. Redrawn from Silk et al. (1986) Spatial Distributions of Potassium, Solutes, and Their Deposition Rates in the Growth Zone of the Primary Corn Root. Plant Physiology 82: 853–858, www.plantphysiol.org, Copyright American Society of Plant Biologists

K^+ as the root ages—compare the younger and older roots. And yet the deposition rate profile shows clearly that potassium is deposited rapidly in the growth zone. The rate of 30 μmoles g^{-1} h^{-1} in much of the growth zone is 14 times the average rate of K uptake reported for entire young maize roots in the field (Mengel and Barber 1974), and 28 times the average flux into hydroponically grown maize roots (Claassen and Barber 1974). The positive deposition rate indicates the growth zone is a large sink for metabolites. Surprisingly this is true even for potentially toxic heavy metals, copper and zinc (Shi et al. 2009). The large sink activity of growth zones is only apparent when the growth dilution term is taken into account

Monocot leaves also have developmental gradients and stage-specific patterns of mineral element deposition. Successively initiated maize leaves have somewhat different profiles of mineral elements. Nevertheless it is evident that growing tissue has the most rapid deposition rate and is the strongest sink for mineral elements (Table 1, from data of Meiri et al. 1992). Although local net deposition rates may be slow, continuing addition or removal of minerals may lead to significant local changes over time. The elements Ca and P in particular accumulate in leaf tips of older maize leaves, as indicated in Table 1 (Meiri et al. 1992).

the tip. Apparently growth- associated water up-take and dry matter production are greater than potassium deposition, so potassium is diluted as cells become longer. Also, each location has less

Regulation of metabolite concentration depends on net deposition rate, not concentration In the example above (Fig. 7), an experimenter seeking to understand potassium transport should look for carrier activity or

Table 1 Deposition rates of nutrients in developing corn leaves

Leaf Serial #	Elongation Rate (mm h^{-1})	Length of growth zone (mm)	Tissue location	Element deposition rate			
				K	Mg	Ca	P
8	3	90	45 mm from node (rapid growth)	740	54	28	3,940
6	1.5	50	100 mm from tip (not growing)	10	0.3	8	410

The leaves were sampled when leaf #8 had emerged from the sheathing base and the older leaf #6 was slowing its growth. Element deposition rates are in neq cm^{-1} h^{-1} (K, Mg, Ca) or ng cm^{-1} h^{-1} (P). Deposition rates for all mineral elements are highest in the expanding tissue near the node, although deposition continues near the tip so that Ca and P concentrations increase there over several plastochrons after the leaf stops growing. (Data from Meiri et al. (1992) Growth and deposition of inorganic nutrient elements in developing leaves of zea-mays L. Plant Physiology 99: 972–978 www.plantphysiol.org, Copyright American Society of Plant Biologists)

up-regulation of gene expression associated with deposition rate. On the other hand, the physiological importance of potassium (as osmoticum for instance) is related to the concentration itself.

N is deposited rapidly into dividing and elongating leaf cells of fescue; RuBisCO in maturing tissue is formed by cannibalization of previously formed metabolites Ecologists know that in the biosphere the bulk of fixed nitrogen is found in leaf chloroplasts in the protein of carbon-fixing enzymes—RuBisCO. Molecular biologists are aware of the fundamental importance of nitrogen in nucleic acids—DNA and RNA. Gastal and Nelson (1994) linked these two aspects of the nitrogen cycle when they calculated N deposition rates in growing fescue leaves (*Festuca arundinacea* Schreb.) (Fig. 8a). Leaf nitrogen concentration was highest in the meristem and elongation zone at the leaf base and fell quickly to a rather constant amount at the end of the growth zone (determined to be about 30 mm long) and in mature tissues. This indicates that nitrogen deposition is rapid in the growth zone and negligible after growth ceases. Nitrate reductase activity (Fig. 8a) and RuBisCO content (Fig. 8b) increased from negligible amounts to a peak beyond the growth zone. Gastal and Nelson thus showed that RuBisCO and other chloroplast proteins in maturing tissue are synthesized from catabolism of compounds formed earlier during cell production and elongation.

Comparison of endogenous deposition rates and exogenous influx reveals contrasting import/export patterns for ammonium and nitrate in growth zones of maize roots Uptake of nitrogen from soil as either nitrate or ammonium is one of the most important root functions. Bloom and colleagues (Colmer and Bloom 1998; Bloom et al. 2002) measured spatial patterns of uptake of NO_3^- and NH_4^+ from the bathing medium, "exogenous influx," by observing with ion-specific electrodes the depletion of these ions in the boundary layer next to the root. They found that when nitrogen was supplied as NH_4NO_3, net influx of NH_4^+ was rather uniform (~1.4 nmol mm^{-1} h^{-1}) through the root cap and root growth zone (Fig. 9). When nitrogen was supplied as $Ca(NO_3)_2$, the pattern of nitrogen influx was significantly different: net NO_3^- influx increased from 1.5 nmol mm^{-1} h^{-1} in the root cap to higher values, 5.4 and 7.6 nmol mm^{-1} h^{-1} at 3.5
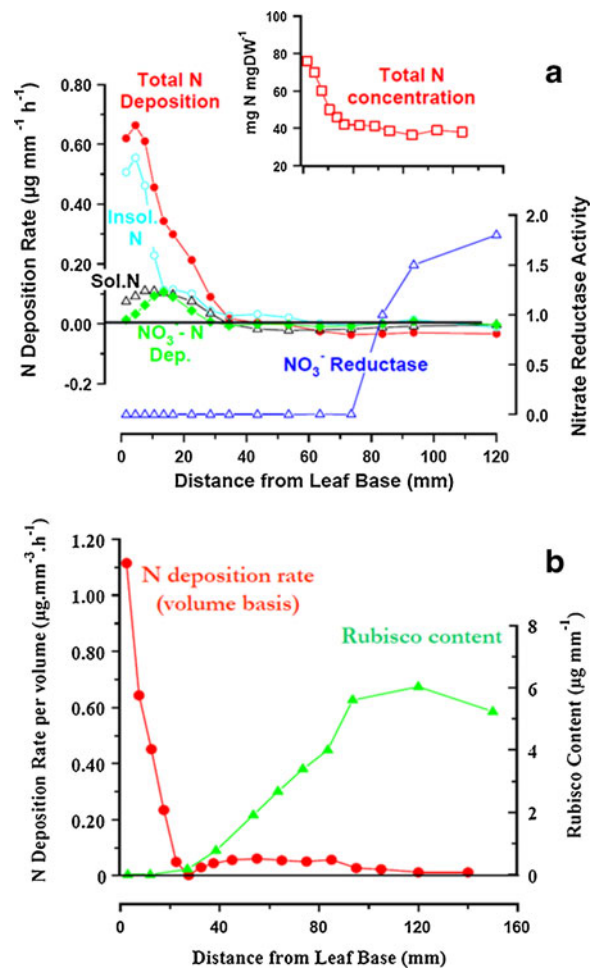

Fig. 8 **a** Profiles of leaf nitrogen content in fescue leaves (inset, top right). Deposition rates of total, insoluble, and soluble N and NO_3-N and nitrate reductase activity. **b** Volumetric N deposition rate superimposed on profile of RuBisCO content. (Adapted from Gastal and Nelson 1994, kindly provided by François Gastal)

and 11 mm, respectively, from the root apex (Fig. 9). Thus the presence of NH_4^+ inhibited net NO_3^- influx. This inhibition together with the observed pattern of H+ fluxes indicated that the entire maize root apex absorbed more exogenous NH_4^+ than NO_3^- when both forms were present in the medium. This makes sense, as assimilation of NH_4^+ costs less energy than NO_3^-. The root is located far from the photosynthetic organs and is energetically starved relative to the shoot. Assimilation of NO_3^- to glutamine expends 12 ATP equivalents versus only 2 ATP equivalents for NH_4^+ to glutamine.

Bloom et al. (2012) then were able to infer the patterns of import and export of different forms of
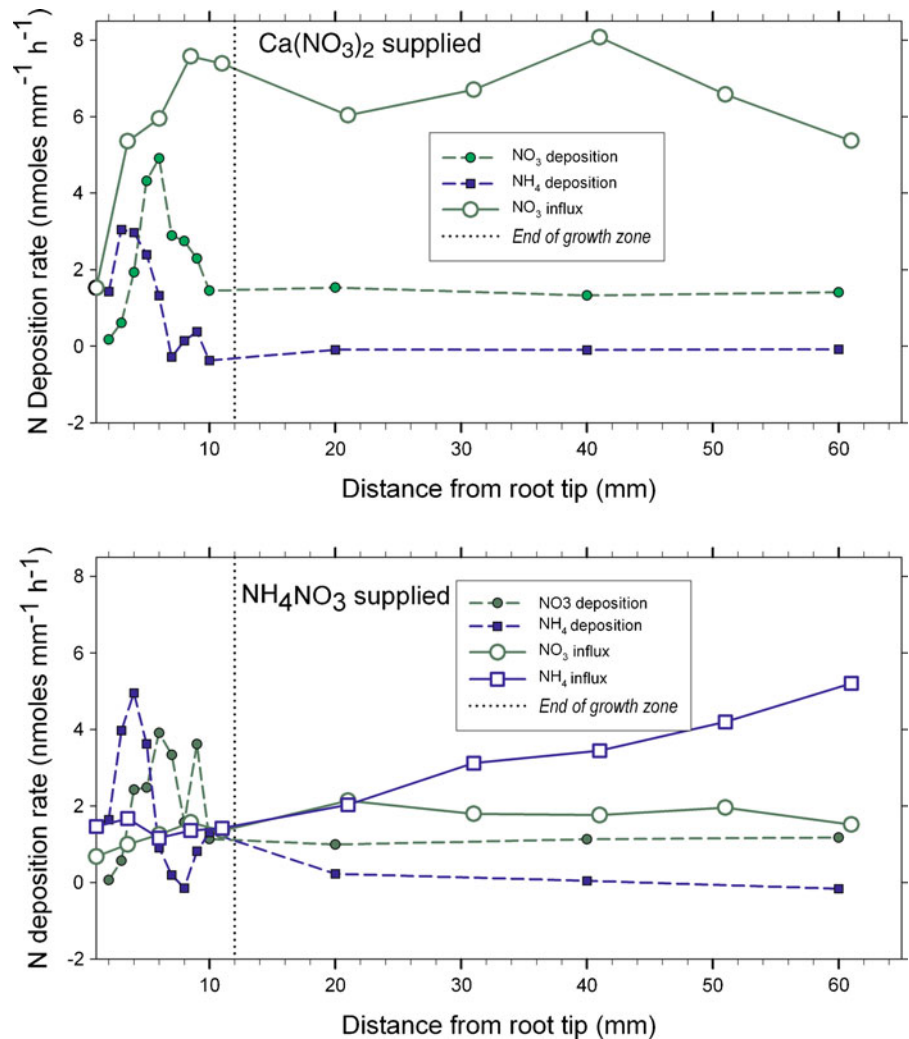
nitrogen by calculating endogenous nitrogen depo-
sition rates and comparing these to the previously
determined exogenous uptake rates (Fig. 9). Where
local deposition exceeds local influx, the tissue
must be importing endogenous nitrogen. Under
$Ca(NO_3)_2$ supply, root NO_3^- influx was adequate
to account for pools found in the growth zone and
provided twice as much as was deposited locally
throughout the non-growing tissue. Some NH_4^+
was deposited and must have been imported from
the seed or shoot. In contrast, under NH_4NO_3
supply, NO_3^- influx was less than the local depo-
sition of NO_3^- in the growth zone, indicating that
additional NO_3^- was imported or metabolically
produced. Yet the profile of NO_3^- in the growth
zone was similar for the plants receiving $Ca(NO_3)_2$

or NH_4NO_3 (Bloom et al. 2012). For both N
supplies, tissue nitrate levels increased from the
meristem through the growth zone and all of the
apical 60 mm. Xylem sap NH_4^+ concentrations
were indifferent to the presence of NO_3^- in the
medium. Since the exogenous uptake of NO_3^- in
the root apex is highly dependent on the presence
of NH_4^+ in the medium, when NH_4^+ is present, all
the NO_3^- absorbed near the apex is stored as free
NO_3^- in the tissues, and additional nitrate is
imported or metabolically produced. When NO_3^-
is the sole N-source, the roots store similar
amounts of free NO_3^- and they absorb additional
NO_3^- that is assimilated or translocated to the
shoot. These results show that NO_3^- deposition,
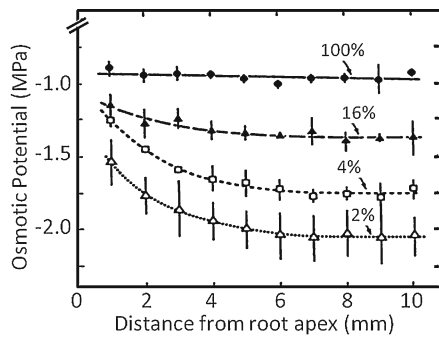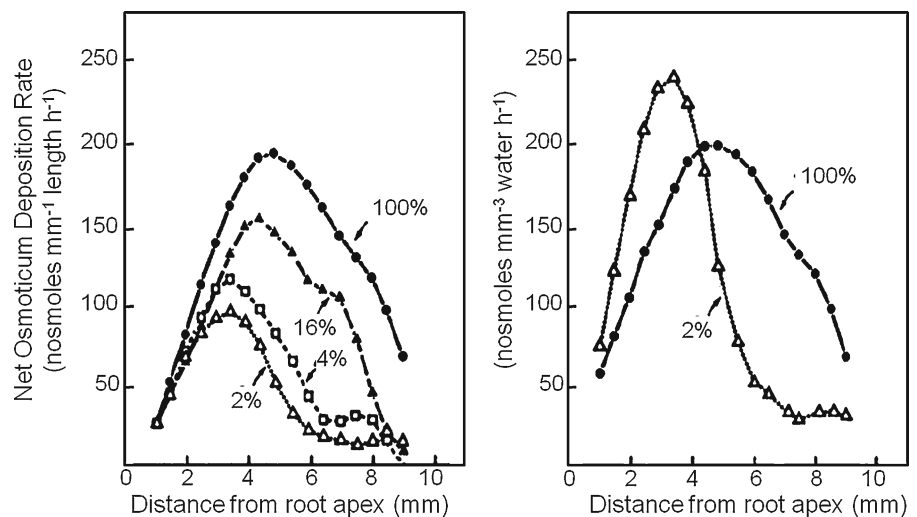whether exogenously supplied or imported, is

Fig. 10 Spatial distribution of osmotic potential in the apical 10 mm of roots growing in vermiculite of various water contents. The treatments represent the vermiculite water content as percentages of the water content at high water potential. Osmotic potentials are means±1 SD from three to seven experiments. From Sharp et al. (1990) Growth of the maize primary root at low water potentials. II. Role of growth and deposition of hexose and potassium in osmotic adjustment. Plant Physiology 93: 1337–1346, www.plantphysiol.org, Copyright American Society of Plant Biologists

important for supporting root elongation in the basal part of the growth zone and maintaining root function in the young mature tissues.

In a related study, Walter and colleagues (2003) determined the endogenous fluxes and deposition rates of metabolites in the seedling roots of maize. They showed that nitrates, but not other nutrients, were exported to a great extent from the root growth zone to the mature tissue. Overall, their results show that a careful analysis of growth kinematics allows quantifying and interpreting a number of important flux parameters in the growing organ.

Biological outcomes: Metabolite deposition rate and growth response to environment

Under water stress, if maize roots do not experience a change in mechanical impedance, osmotic adjustment occurs with decreased rates of solute deposition coupled to larger decreases in radial growth rates In plants subjected to water deficit turgor may be maintained by true osmotic adjustment, which consists of decreasing cell osmotic potential by increased solute content without change of relative water content. In growing tissue, osmotic adjustment can result from either osmoticum accumulation or reduced tissue volume expansion. In maize seedlings submitted to different levels of water deficit, the osmotic potential along the root apex decreased in proportion to the stress level while relative water content was weakly affected, indicating true osmotic adjustment (Fig. 10) (Sharp et al. 1990). Based on osmotic potential and water content profiles, the net deposition rates of osmoticum were calculated using the continuity equation (Eq. 1C), per unit length and per unit volume. While the net deposition rate relative per mm decreased over most of the root tip in response to water deficit, the net deposition rate relative to volume increased in the apical part of the apex (Fig. 11). This happens because root radius and water content per unit length were strongly decreased by the water deficits all along the growth zone (Sharp et al. 1988, 1990). Thus, the drought-induced decrease of radial root growth allowed substantial osmotic adjustment despite reduced solute

Fig. 11 Spatial distribution of net deposition rates of osmoticum in the apical 10 mm of roots growing at the various vermiculite relative water contents. Citation as for Fig. 10

deposition and contributed to the maintenance of primary root elongation in the three apical millimetres. This highlights the importance of considering growth in all dimensions (and not only the main strain direction), especially when comparing among treatments. The comparison of the net deposition rate of hexoses, known to be involved in osmotic adjustment, with that of potassium, a major mineral component of cell sap, showed that hexoses contributed to osmotic adjustment while potassium did not: solute net deposition rates were species-dependent and uncoupled from volumetric growth.

Similar conclusions were found in growing leaves of tall fescue after water was withheld (Spollen and Nelson 1994). The increasing levels of water deficit reduced the relative elemental elongation rates and shortened the growing zone in proportion to the duration of water withholding. When the water deficit exceeded a threshold, the dry matter content per unit length was increased by more than 20 % over the whole growing zone while leaf elongation rate was decreased by approximately 50 %, indicating that net dry matter import rate must have been decreased in this growing zone. Further analyses of water soluble carbohydrates content suggested that the hydrolysis of fructan stored in the distal part of the elongation zone could account for an increased content in hexoses in the apical part. It is clear that the accumulation of water soluble carbohydrates leads to osmotic adjustment.

We note that these effects of drought occurred only in the absence of changes in soil hardness. In contrast roots often grow thicker in those soils that become hard to penetrate as they dry. (reviewed in Bengough et al. 2006). Work remains to analyze the growth kinematics and metabolism as the root adapts to increased soil impedance.

In salt-affected sorghum leaves, decreases in potassium deposition rates parallel decreases in growth rates Bernstein et al. (1995) analyzed growth and mineral deposition rates in leaves of sorghum (*Sorghum bicolor* [L.] Moench, cv. 'NK 265') plants grown in nutrient solution with and without 1,000 mol m^{-3} NaCl salinity. Salinity affected both growth and mineral content. The relative elemental growth rate and water deposition rates were not much affected in the proximal

meristematic regions and were progressively more inhibited toward the base of the growth zone (Fig. 12a). Salinity produced elevated concentrations of Na and decreased concentrations of K and Ca; while Mg deposition rates were synchronized with water deposition rates so that tissue concentrations of Mg were not much affected by salinity. The decrease in Ca deposition rate relative to control was uniform along the growth zone (Fig. 12b). In contrast the K deposition rate was more strongly affected in distal regions (Fig. 12c). The parallel inhibitions of growth and K deposition rate suggest the latter might be particularly important in regulating the growth response to salinity.

Aphid infestation of alfalfa transforms apical nitrate sink tissue to a nitrate source Girousse and colleagues (2005) studied carbon and nitrogen deposition in alfalfa (*Medicago sativa* L.) infested by a pea aphid. This aphid is a phloem feeder that does not transmit virus or toxins, and assimilate withdrawal is
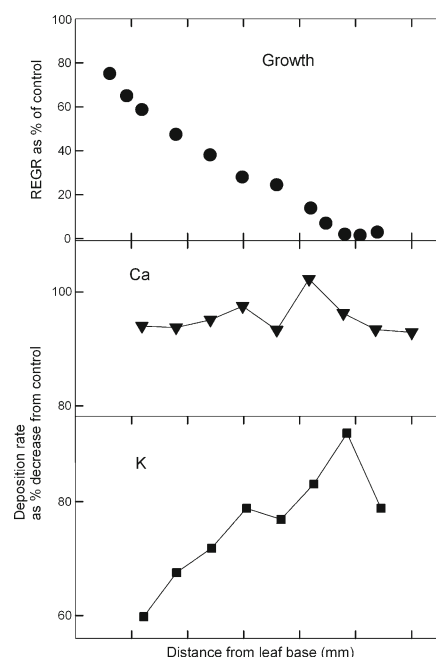

Fig. 12 Salinity effects on the relative elemental growth rate (top graph), calcium deposition rate (middle graph) and potassium deposition rate (bottom graph) as compared to control. Redrawn from Bernstein et al. (1995) Growth and development of sorghum leaves under conditions of NaCl stress - possible role of some mineral elements in growth-inhibition. Planta 196: 699–705 with kind permission of Springer Science+Business Media
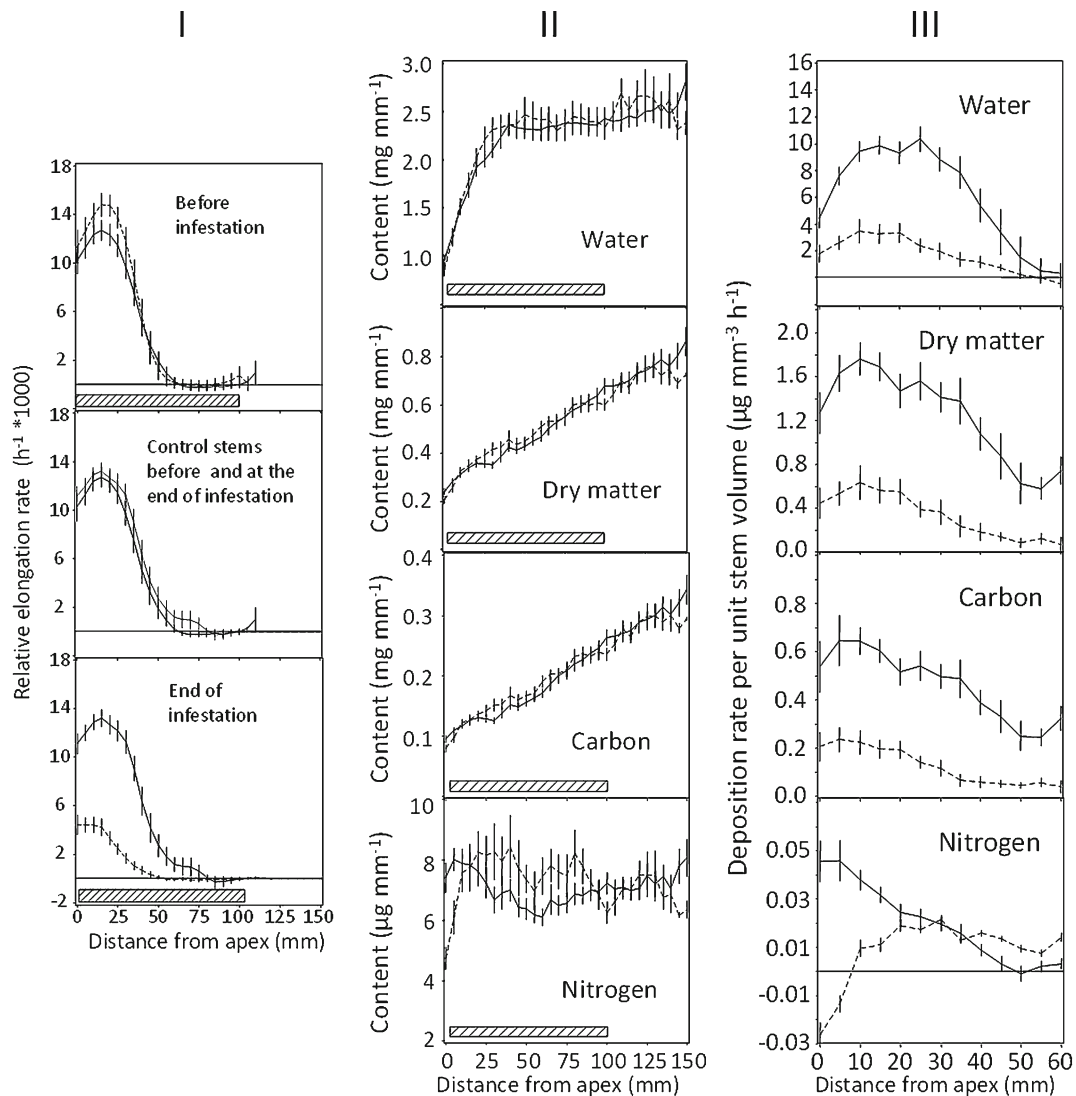
Fig. 13 Effect of aphid infestation on spatial patterns of (I) growth, (II) water, dry matter, carbon, and nitrogen, and (III) deposition rates of water, dry matter, carbon, and nitrogen in alfalfa stems. Adapted from Girousse et al. (2005) Aphid infestation causes different changes in carbon and nitrogen allocation in alfalfa stems as well as different inhibitions of longitudinal and radial expansion. Plant Physiology 137: 1474–1484, www.plantphysiol.org, Copyright American Society of Plant Biologists; kindly provided by Christine Girousse

generally considered as the main mechanism responsible for growth reduction. Girousse et al. found that severe short-term aphid infestation (200 young adults over a 24-h period) induced a strong reduction in growth rate, particularly longitudinal expansion (Fig. 13-I). Profiles of carbon and dry matter were unaffected by the infestation, indicating that the growth reductions were synchronized with reductions in deposition rates of water and carbon (Fig. 13-II). However the aphid effects on plant nitrogen were quite different. Reduced nitrogen content and associated negative nitrogen deposition rates (Fig. 13-III) were observed in the apex. This indicated a mobilization of nitrogen from the apical part of the growth zone, converted from a sink tissue into a source tissue by aphids. From the growth anisotropy the authors were also able to conclude that aphid-induced thigmotropism is associated with the long term effects of the infestation.

Molecular biology: Utility and outcomes

In mature tissues, where cells do not enlarge, the transcriptional regulation of gene expression (e.g., environmental induction) is computed as the temporal change of transcript density in a stationary reference frame. In practice, gene induction or repression is inferred from the ratio of the gene expression in treated plants relative to controls. When focusing on development, gene expression is compared in samples collected in different positions representative of successive time points. For instance, highly accurate maps of gene expression in the root apex have been produced, highlighting coordinated gene expression networks (Birnbaum et al. 2003; Brady et al. 2007). Since longitudinal profiles describe the different developmental stages undergone by a cell during growth, one could be tempted to deduce regulation of gene expression from variations of gene expression along the growing zone. However, this would be misleading since cells expand at varying rates while being displaced along the root. The continuity equation can be used with growth trajectories to get an unbiased view of the spatio-temporal regulation of gene expression.

Actin11 is highly regulated by a balance of transcription and decay during growth of poplar roots This framework has recently been used to analyze the regulation of gene expression within the growing zone of the root. Merret et al. (2010) determined transcript densities and calculated rates of change in gene expression and molecular developmental information in the poplar root apex. The authors focused on two genes widely used as internal control in real-time qPCR (Brunner et al. 2004), *Actin11* and *Elongation*

Factor 1-β (*EF1β*). Gene expression was quantified at high spatial resolution with real time PCR. The *Actin11* transcript density profile displayed two peaks at 1.5 and 3.5 mm from the root tip with similar spans but decreasing intensity, and low values in more distal segments (Fig. 4). The net accumulation rate of transcript reveals the regulation of gene expression resulting from the balance of transcription and decay along the root, corrected for the positional and dilutive effects of growth (Fig. 14a). Positive rates denote upregulation while negative rates denote downregulation, it was shown that *Actin11* expression profile resulted from highly controlled regulation. The drawing of the Lagrangian specification also highlighted that the high expression level in the segment [1–2 mm] is produced by a quite small but longlasting induction and that classical spatial specifications hide temporal aspects of regulation (Fig. 14b). This work showed that this gene cannot be used as reference gene for normalization in real time PCR when developing organs are considered.

While gene expression is usually normalized in order to get rid of sampling error and to eliminate differences of biological activity among samples, the continuity equation must be applied to absolute quantities, thus on transcript densities. Since the density of nuclei and presumably the cellular activity are heterogeneous along the root growth zone, net accumulation rates must be compared to the net accumulation rate of a standard entity, either the expression of reference genes or cell density. Merret and co-authors used total RNA content as an estimate of cell density (2010). As expected, the net accumulation rate of total RNA was
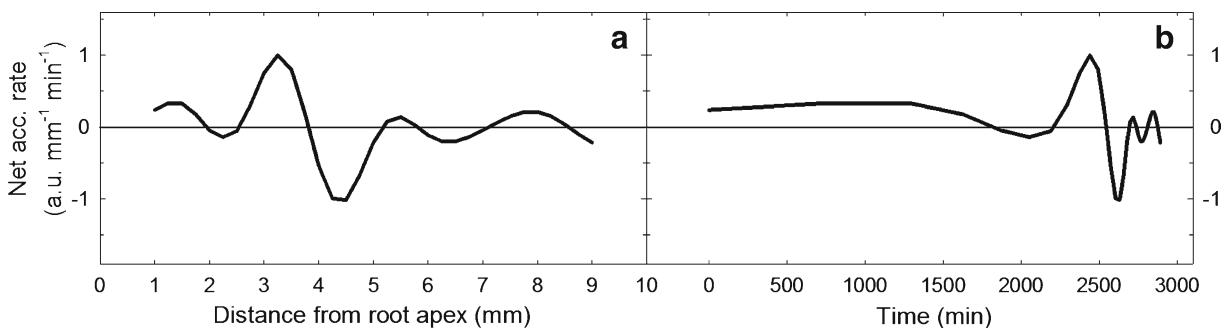

Fig. 14 a Net accumulation rate of *Actin11* transcripts as a function of the distance from the root tip (Eulerian specification), expressed in arbitrary unit mm^{-1} min^{-1} and calculated using Eq. (1A). **b** Net accumulation rate of *Actin11* transcripts as a function of the time for a particule starting at 1 mm at $t=$ 0 (Lagrangian specification) (redrawn from Merret et al. 2010)

null, except in the meristem supporting the significance of the conclusions about the regulation of *Actin 11* expression (Merret et al. 2010).

A model shows the regulatory importance of hormone dilution by plant growth Recently, a modelling approach has suggested that growth-induced dilution of gibberellins (GA) can explain the dynamics of cell elongation in the *Arabidopsis thaliana* root apex (Band et al. 2012). Assuming that all parameters are steady, the model uses cell diameter, cell length profile along the growing zone and root growth rate to describe the volume increase of a growing cell in space and time, that is, in a Lagrangian way. The model also takes into account the biochemical rules determining hormone transfer among four subcellular compartments: the vacuole, nucleus, cytoplasm and cell wall. Based on transcriptomics and reporter analysis, GA biosynthesis and degradation are supposed to be null in the elongation zone. So, the model estimates the GA concentration in the cell during its expansion and predicts a significant growth-induced dilution. In parallel, the concentration of components belonging to the signalling networks, including the gibberellin receptor GID1 and the well-known growth repressing DELLA proteins, are calculated from the corresponding measured mRNA levels and the cell dimensions. Then, the molecular mechanism regulating the amount of DELLA proteins are incorporated in the model (To simplify, each gene family is treated as a single representative species). The multiscale model shows that the declining GA concentration along the elongation zone affects the level of downstream signalling components, in particular increases the concentration of DELLA proteins, which in turn decreases the relative cell elongation, implying a feedback loop. These implications were tested and confirmed through the phenotyping of roots treated with paclobutrazol (inhibiting GA biosynthesis) and GA biosynthetic mutants. This study also reveals that even if *DELLA* expression level appears constant over the duration of cell elongation, the protein level can vary, controlled by its degradation rate, which depends on the GA concentration. Authors note the importance of growth-induced GA dilution as cells pass through the elongation zone as a key finding in the control of cell elongation.

Deposition rates of GA regulate growth of maize leaves Deposition rates of gibberellins have recently been shown to have an important role in regulating growth of maize leaves. Nelissen et al. (2012) made direct measurements of endogeneous hormone concentrations in the maize leaf growth zone and showed that the bioactive GA_1 peaks in the transition zone at the distal end of the cell division zone. Using the continuity equation they showed that GA_1 accumulation rate is positive in the division zone and the proximal part of the transition zone but drops very rapidly to negative values at the entrance in the strictly-elongation zone, highlighting that, in this zone, catabolic activity and/or export take place in addition to dilution. The combined metabolic and transcriptomic profiling revealed that the GA maximum is established by GA biosynthesis in the division zone and active GA catabolism at the onset of the expansion-only zone. Use of mutants deficient in GA and transgenic plants that overproduce GA confirmed that the size of the cell division zone varies with the GA deposition rate.

Fluorescent tagging of cell membranes and nuclei combined with automated particle tracking may greatly facilitate calculation of deposition rates in plant organs Recently, powerful computational techniques have been disseminated to allow automated particle tracking so that cell cohorts are followed through space and time. An exciting approach, which the authors have called *in planta* cytometry, allows automated, nondestructive analysis of both growth and spatial patterns of gene expression (Federici et al. 2012). Nuclei were labeled with one fluorescent protein, and membranes were labeled with another; cells imaged with confocal microscopy then had red nuclei and blue edges. Using a particle search algorithm index cells were followed in space and time. Federici and colleagues then wrote an active contour segmentation algorithm that allowed them to quantify cell and shape and hence growth strain rates. These numerical methods are now available for use with the Image J platform (maintained by NIH). Then cell-specific gene expression was quantified by ratiometric measurement of spectrally distinct nuclear fluorescent proteins expressed under the control of differently regulated promoters. This paper implies that automated high-throughput technology is now available to analyze many aspects of growth kinematics in experimental systems

that can be genetically transformed. In particular, the coming decade should reveal many cell-specific (Lagrangian) descriptions of deposition rates and inclusion of dilutional and positional effects to identify gene regulation causing organ development.

Conclusions

The continuity equation, used with empirical data on growth velocity and concentration, allows computation of biosynthesis and deposition rates in growing tissue. These deposition rates give important insight into the mechanism of plant response to drought and salinity, and they clarify many aspects of nitrogen metabolism in roots and leaves. This approach is also essential to understand molecular regulation of growth. Models of the molecular biology underlying plant development are still dominated by time-dependent formulations that are inadequate because they neglect cell displacement and expansion. However several pioneering studies have incorporated growth analysis into well-designed experiments to discover the kinematics of gene regulation. And new technologies—*in planta* cytometry, coupled with powerful new computational routines and real-time confocal microscopy—promise advancement in understanding of gene regulation in growing organs, especially in those systems that can be transformed with fluorescent tags.

References

Band LR, Ubeda-Tomas S, Dyson RJ, Middleton AM, Hodgman TC, Owen MR, Jensen OE, Bennett MJ, King JR (2012) Growth-induced hormone dilution can explain the dynamics of plant root cell elongation. Proc Natl Acad Sci U S A 109:7577–7582

Beemster GTS, Baskin TI (1998) Analysis of cell division and elongation underlying the developmental acceleration of root growth in *Arabidopsis thaliana*. Plant Physiol 116:1515–1526

Bengough AG, Bransby MF, Hans J, McKenna SJ, Roberts TJ, Valentine TA (2006) Root responses to soil physical conditions; growth dynamics from field to cell. J Exp Bot 57:437–447

Bernstein N, Silk WK, Lauchli A (1995) Growth and development of sorghum leaves under conditions of NaCl stress—possible role of some mineral elements in growth-inhibition. Planta 196:699–705

Birnbaum K, Shasha DE, Wang JY, Jung JW, Lambert GM, Galbraith DW, Benfey PN (2003) A gene expression map of the Arabidopsis root. Science 302:1956–1960

Bloom AJ, Meyerhoff PA, Taylor AR, Rost TL (2002) Root development and absorption of ammonium and nitrate from the rhizosphere. J Plant Growth Regul 21:416–431

Bloom AJ, Randall L, Taylor AR, Silk WK (2012) Deposition of ammonium and nitrate in the roots of maize seedlings supplied with different nitrogen salts. J Exp Bot 63:1997–2006

Boas ML (2005) Mathematical methods in the physical sciences. John Wiley & Sons, p 864

Boffey SA, Sellden G, Leech RM (1980) Influence of cell age on chlorophyll formation in light-grown and etiolated wheat seedlings. Plant Physiol 65:680–684

Brady SM, Orlando DA, Lee J-Y, Wang JY, Koch J, Dinneny JR, Mace D, Ohler U, Benfey PN (2007) A high-resolution root spatiotemporal map reveals dominant expression patterns. Science 318:801–806

Brunner AM, Busov VB, Strauss SH (2004) Poplar genome sequence: functional genomics in an ecologically dominant plant species. Trends Plant Sci 9:49–56

Claassen N, Barber SA (1974) Method for characterizing relation between nutrient concentration and flux into roots of intact plants. Plant Physiol 54:564–568

Colmer TD, Bloom AJ (1998) A comparison of NH_4^+ and NO_3^- net fluxes along roots of rice and maize. Plant Cell Environ 21:240–246

Cunha A, Tarr PT, Roeder AHK, Altinok A, Mjolsness E, Meyerowitz EM (2012) Computational analysis of live cell images of the *Arabidopsis thaliana* plant. In: Asthagiri AR, Arkin AP (eds) Computational methods in cell biology. Elsevier Academic Press Inc, San Diego, pp 285–323

Erickson RO (1966) Relative elemental rates and anisotropy of growth in area—a computer programme. J Exp Bot 17:390

Erickson RO (1976) Modeling of plant-growth. Annu Rev Plant Physiol Plant Mol Biol 27:407–434

Erickson RO, Sax KB (1956) Elemental growth-rate of the primary root of *Zea-mays*. Proc Am Philos Soc 100:487–498

Federici F, Dupuy L, Laplaze L, Heisler M, Haseloff J (2012) Integrated genetic and computation methods for in planta cytometry. Nat Methods 9:483–U104

Fiorani F, Beemster GTS (2006) Quantitative analyses of cell division in plants. Plant Mol Biol 60:963–979

Gandar PW (1983a) Growth in root apices. I. The kinematic description of growth. Bot Gaz 144:1–10

Gandar PW (1983b) Growth in root apices. II. Deformation and rate of deformation. Bot Gaz 144:11–19

Gastal F, Nelson CJ (1994) Nitrogen use within the growing leaf blade of tall fescue. Plant Physiol 105:191–197

Girousse C, Moulia B, Silk W, Bonnemain JL (2005) Aphid infestation causes different changes in carbon and nitrogen allocation in alfalfa stems as well as different inhibitions of longitudinal and radial expansion. Plant Physiol 137:1474–1484

Goodwin RH, Stepka W (1945) Growth and differentiation in the root tip of *Phleum pratense*. Am J Bot 32:36–46

Grandjean O, Vernoux T, Laufs P, Belcram K, Mizukami Y, Traas J (2004) In vivo analysis of cell division, cell growth, and differentiation at the shoot apical meristem in Arabidopsis. Plant Cell 16:74–87

Green PB (1976) Growth and cell pattern formation on an axis—critique of concepts, terminology, and modes of study. Bot Gaz 137:187–202

Koehl MAR, Silk WK, Liang H, Mahadevan L (2008) How kelp produce blade shapes suited to different flow regimes: a new wrinkle. Integr Comp Biol 48:834–851

Kwiatkowska D, Dumais J (2003) Growth and morphogenesis at the vegetative shoot apex of *Anagallis arvensis* L. J Exp Bot 54:1585–1595

Meiri A, Silk WK, Lauchli A (1992) Growth and deposition of inorganic nutrient elements in developing leaves of *Zea mays* L. Plant Physiol 99:972–978

Mengel DB, Barber SA (1974) Rate of nutrient uptake per unit of corn root under field conditions. Agron J 66:399–402

Merret R, Moulia B, Hummel I, Cohen D, Dreyer E, Bogeat-Triboulot MB (2010) Monitoring the regulation of gene expression in a growing organ using a fluid mechanics formalism. BMC Biol 8:18

Miller ND, Parks BM, Spalding EP (2007) Computer-vision analysis of seedling responses to light and gravity. Plant J 52:374–381

Nelissen H, Rymen B, Jikumaru Y, Demuynck K, Van Lijsebettens M, Kamiya Y, Inze D, Beemster GTS (2012) A local maximum in gibberellin levels regulates maize leaf growth by spatial control of cell division. Curr Biol 22:1183–1187

Reddy GV, Heisler MG, Ehrhardt DW, Meyerowitz EM (2004) Real-time lineage analysis reveals oriented cell divisions associated with morphogenesis at the shoot apex of *Arabidopsis thaliana*. Development 131:4225–4237

Schnyder H, Nelson CJ (1988) Diurnal growth of tall fescue leaf blades.1. Spatial-distribution of growth, deposition of water, and assimilate import in the elongation zone. Plant Physiol 86:1070–1076

Sharp RE, Hsiao TC, Silk WK (1990) Growth of the maize primary root at low water potentials. II. Role of growth and deposition of hexose and potassium in osmotic adjustment. Plant Physiol 93:1337–1346

Sharp RE, Silk WK, Hsaio TC (1988) Growth of the maize primary root at low water potentials. I. Spatial distribution of expansive growth. Plant Physiol 87:50–57

Shi JY, Gras MA, Silk WK (2009) Laser ablation ICP-MS reveals patterns of copper differing from zinc in growth zones of cucumber roots. Planta 229:945–954

Silk WK (1984) Quantitative descriptions of development. Annu Rev Plant Physiol 35:479–518

Silk WK, Erickson RO (1978) Kinematics of hypocotyl curvature. Am J Bot 65:310–319

Silk WK, Erickson RO (1979) Kinematics of plant-growth. J Theor Biol 76:481–501

Silk WK, Hsiao TC, Diedenhofen U, Matson C (1986) Spatial distributions of potassium, solutes, and their deposition rates in the growth zone of the primary corn root. Plant Physiol 82:853–858

Silk WK, Lord EM, Eckard KJ (1989) Growth-patterns inferred from anatomical records—empirical tests using longisections of roots of Zea-mays-L. Plant Physiol 90:708–713

Silk WK, Walker RC, Labavitch J (1984) Uronide deposition rates in the primary root of *Zea mays*. Plant Physiol 74:721–726

Spollen WG, Nelson CJ (1994) Response of fructan to water-deficit in growing leaves of tall fescue. Plant Physiol 106:329–336

Tardieu F, Granier C, Muller B (2011) Water deficit and growth. Co-ordinating processes without an orchestrator? Curr Opin Plant Biol 14:283–289

Triboulot MB, Pritchard J, Tomos D (1995) Stimulation and inhibition of pine root growth by osmotic stress. New Phytol 130:169–175

Walter A, Feil R, Schurr U (2003) Expansion dynamics, metabolite composition and substance transfer of the primary root growth zone of *Zea mays* L. grown in different external nutrient availabilities. Plant Cell Environ 26:1451–1466

Walter A, Spies H, Terjung S, Kusters R, Kirchgessner N, Schurr U (2002) Spatio-temporal dynamics of expansion growth in roots: automatic quantification of diurnal course and temperature response by digital image sequence processing. J Exp Bot 53:689–698